Article

Production of Jets at STAR

Michal Svoboda [1,2]
for the STAR Collaboration

[1] Nuclear Physics Institute, Czech Academy of Sciences; m.svoboda@ujf.cas.cz
[2] Department of Physics, Faculty of Nuclear Sciences and Physical Engineering, Czech Technical University in Prague

Abstract: Jets serve as an important tool to probe QCD both in the vacuum and in the hot and dense medium. The STAR experiment at RHIC plays a key role in studying QCD phenomena across different collision systems (p+p, p+A, A+A), offering access to a kinematic regime that complements that of the LHC. Building on recent jet and event activity studies at STAR, we present recent measurements on charged-particle jets at $\sqrt{s_{\mathrm{NN}}} = 200$ GeV. In p+Au collisions, we explore event activity (EA) measured in the Au-going direction and its correlation with particle production at mid-rapidity. While soft particle production increases with EA, high-p_{T} jets are found to be inversely related to EA. Ratios of p_{T} imbalance and azimuthal dijet separation between high- and low-EA events show no significant differences, suggesting no strong evidence of jet quenching in high-EA p+Au collisions. In Au+Au collisions, we report semi-inclusive measurements of jets recoiling from γ and π^0 triggers, using mixed-event techniques to subtract background and study jet suppression, intra-jet broadening, and acoplanarity. Additionally, we present inclusive charged-particle jet spectra corrected for background fluctuations, extending the kinematic reach of previous measurements. These results provide crucial insight into the modification of jets in the medium and contribute to a deeper understanding of QCD in heavy-ion collisions.

Keywords: jet, STAR, charged-particle jet, semi-inclusive jet

1. Introduction

Shortly after the Big Bang, the Universe existed in a unique state of matter known as the Quark-Gluon Plasma (QGP), where quarks and gluons were no longer confined within hadrons but formed a hot, dense medium. This state of matter can be recreated for a brief moment in high-energy heavy-ion collisions at large-scale particle colliders such as the Large Hadron Collider (LHC) at CERN and the Relativistic Heavy Ion Collider (RHIC) in the USA.

One of the primary tools to study the QGP is the measurement of jets—collimated sprays of particles resulting from the fragmentation and hadronization of hard-scattered partons. Jets are produced in both proton-proton ($p + p$) and heavy-ion collisions, making them an excellent probe for exploring the properties of the QGP. By comparing jet properties between $p + p$ and heavy-ion collisions, the modifications induced by the medium can be studied.

A key observable in this context is jet quenching, which refers to the energy loss experienced by high-energy partons as they traverse the QGP. Jet quenching manifests itself through the suppression of high transverse momentum particle yields and modifications to the structure of fully reconstructed jets, providing crucial insight into the interactions between hard probes and the QGP medium.

Received:
Revised:
Accepted:
Published:

Citation: Lastname, F.; Lastname, F.; Lastname, F. Title. *Journal Not Specified* **2025**, *1*, 0. https://doi.org/

2. Experimental Setup

The RHIC is an exceptionally versatile accelerator capable of delivering beams of various species, from protonn to uranium. It operates over a wide range of collision energies, from $\sqrt{s_{\rm NN}}$ = 3 GeV in fixed-target mode up to 200 GeV for ion collisions, and up to 510 GeV for proton-proton ($p + p$) collisions. This versatility is complemented by the STAR detector, which is equipped with multiple subsystems designed for measurements across an extensive kinematic range. A 3D model of the STAR experiment (from 2014) can be seen in Figure 1.

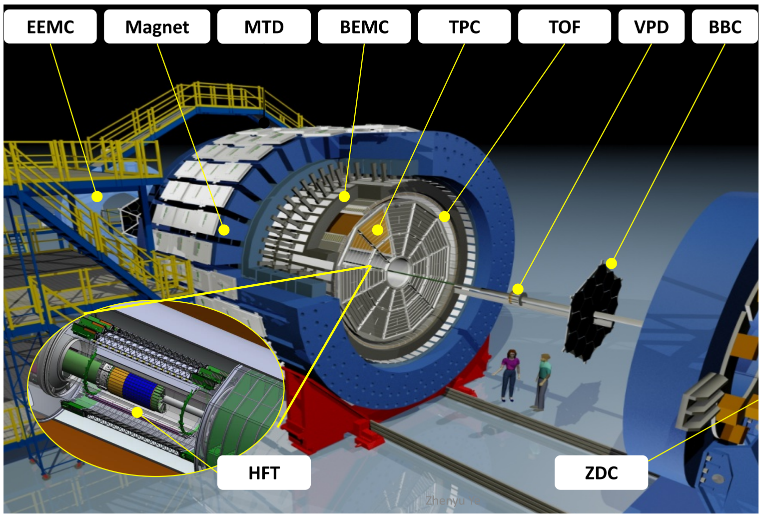

Figure 1. STAR detector and its sub-detectors. Taken from Ref. [1].

The Time Projection Chamber (TPC), covering pseudorapidity $|\eta| < 1$, provides precise tracking and momentum measurement of charged particles. It also serves as a tool for centrality determination through charged-particle multiplicity selection. The Barrel Electromagnetic Calorimeter (BEMC), also at $|\eta| < 1$, detects energy deposits from photons, electrons, and charged hadrons, while additionally functioning as a fast online trigger. The Time-of-Flight (TOF) detector, operating within $|\eta| < 0.9$, identifies particles based on their velocities and plays a role in mitigating pileup events.

At higher rapidities, the Vertex Position Detector (VPD) operates in the range $4.24 < |\eta| < 5.1$, while the Zero Degree Calorimeter (ZDC) is positioned 18 meters downstream. Both serve as minimum bias triggers. Additionally, the VPD contributes to precise vertex reconstruction through its excellent timing capabilities, enhancing position resolution. The ZDC also plays a critical role in monitoring luminosity. Another detector consisting of two parts positioned far from the center of STAR is the Beam-Beam Counter (BBC), which operates in the range $3.4 < |\eta| < 5.0$. It serves as a trigger for $p + p$ collisions and is also used to estimate a proxy for centrality in the p+Au collisions.

3. Results

In the analyses presented here, the jets are reconstructed using the anti-$k_{\rm T}$ algorithm. Two types of jets are considered: charged-particle jets, which are reconstructed solely from charged-particle tracks in the TPC, and full jets, which incorporate both charged-particle tracks from the TPC and energy deposits measured in the BEMC towers. Measurements from two collision systems are presented, $p+$Au and Au $+$ Au collisions. The analyses benefit from a low constituent transverse momentum ($p_{\rm T}$) cut-off of 0.2 GeV/c, which allows for less biased jet reconstruction. Furthermore, the kinematic reach extends to jet transverse momenta of approximately 50–60 GeV/c, enabling meaningful comparisons with the results of the LHC experiments.

3.1. Inclusive Charged-particle Jets in Au+Au Collisions

In Au+Au collisions a strong effect of medium on the jet production is expected. One of the variables, which can be used to study effects of the medium is so called central-to-peripheral ratio R_{CP} defined as

$$R_{\mathrm{CP}} = \frac{\langle N_{\mathrm{coll}}^{\mathrm{per}} \rangle}{\langle N_{\mathrm{coll}}^{\mathrm{cent}} \rangle} \cdot \frac{\frac{1}{N_{\mathrm{evt}}^{\mathrm{AA,cent}}} \frac{\mathrm{d}^2 N_{\mathrm{AA,cent}}^{\mathrm{jet}}}{\mathrm{d}p_{T,\mathrm{jet}} \mathrm{d}\eta}}{\frac{1}{N_{\mathrm{evt}}^{\mathrm{AA,per}}} \frac{\mathrm{d}^2 N_{\mathrm{AA,per}}^{\mathrm{jet}}}{\mathrm{d}p_{T,\mathrm{jet}} \mathrm{d}\eta}}, \tag{1}$$

which compared jet yield measured in central collisions $\frac{\mathrm{d}^2 N_{\mathrm{AA,cent}}^{\mathrm{jet}}}{\mathrm{d}p_{T,\mathrm{jet}} \mathrm{d}\eta}$ scaled by the number of analyzed central events $N_{\mathrm{evt}}^{\mathrm{AA,cent}}$ to the jet yield measured in peripheral collisions $\frac{\mathrm{d}^2 N_{\mathrm{AA,per}}^{\mathrm{jet}}}{\mathrm{d}p_{T,\mathrm{jet}} \mathrm{d}\eta}$ scaled by the corresponding number of events $N_{\mathrm{evt}}^{\mathrm{AA,per}}$. The spectra are also scaled by the average number of binary collisions estimated from the Glauber model for central $\langle N_{\mathrm{coll}}^{\mathrm{per}} \rangle$ and peripheral collisions $\langle N_{\mathrm{coll}}^{\mathrm{cent}} \rangle$. If there were no effects of the QGP medium present, this ratio would be equal to unity.

Figure 2 presents a comparison of R_{CP} for charged-particle jets with $R = 0.2$ and $R = 0.3$ in $\sqrt{s_{\mathrm{NN}}} = 200$ GeV to that measured in the Pb+Pb collisions at $\sqrt{s_{\mathrm{NN}}} = 2.76$ TeV [2] and to the R_{CP} for charged hadrons measured in Au+Au collisions at $\sqrt{s_{\mathrm{NN}}} = 200$ GeV [3] and in Pb+Pb collisions at $\sqrt{s_{\mathrm{NN}}} = 2.76$ TeV [4]. For the Au+Au jet measurements shown, central and peripheral collisions correspond to the 0–10% and 60–80% centrality intervals, respectively. For LHC jet measurements, the corresponding intervals are 0–10% and 50–80%, while for charged hadron measurements at both RHIC and LHC the intervals are 0–5% and 60–80%. The charged-particle jet R_{CP} shows significant suppression in the central collisions compared to the peripheral collisions reaching the value of ~ 0.5 independently of the jet p_{T}.

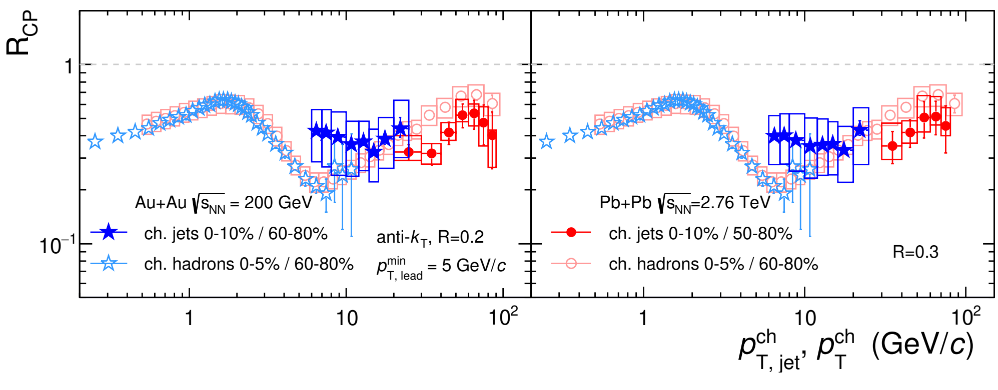

Figure 2. The R_{CP} distributions $(0-10\%/60-80\%)$ for Au+Au collisions at $\sqrt{s_{\mathrm{NN}}} = 200$ GeV compared to those measured in Pb+Pb collisions at $\sqrt{s_{\mathrm{NN}}} = 2.76$ TeV [2] for $R = 0.2$ (left) and $R = 0.3$ (right). Also shown are R_{CP} values for inclusive charged hadrons in Au+Au collisions at $\sqrt{s_{\mathrm{NN}}} = 200$ GeV [3] and in Pb+Pb collisions at $\sqrt{s_{\mathrm{NN}}} = 2.76$ TeV [4]. Data from RHIC are shown in blue, while data from the LHC are shown in red. Taken from Ref. [5].

The R_{CP} values for charged hadrons at RHIC and LHC agree within uncertainties over their common p_{T} range. Similarly, the magnitude of charged-particle jet R_{CP} is consistent within uncertainties between RHIC and LHC, though their $p_{\mathrm{T,jet}}^{\mathrm{ch}}$ intervals do not overlap. The observed lack of $p_{\mathrm{T,jet}}^{\mathrm{ch}}$ dependence for jet R_{CP} contrasts with the significant p_{T} dependence of charged-hadron R_{CP}. This difference reflects the fragmentation process, where the leading hadron carries only part of the parent jet's energy, resulting in different p_{T}-

dependent suppression patterns. Consequently, a comparison of hadron and jet suppression provides important constraints on theoretical models of jet quenching.

Similarly, as R_{CP} compares central and peripheral collisions, the nuclear modification factor R_{AA} is defined to compare collisions of nuclei to the collisions of protons.

$$R_{\mathrm{AA}} = \frac{1}{\langle N_{\mathrm{coll}} \rangle} \cdot \frac{\frac{1}{N_{\mathrm{evt}}^{\mathrm{AA}}} \frac{\mathrm{d}^2 N_{\mathrm{AA}}^{\mathrm{jet}}}{\mathrm{d}p_{\mathrm{T,jet}}\mathrm{d}\eta}}{\frac{1}{N_{\mathrm{evt}}^{pp}} \frac{\mathrm{d}^2 N_{pp}^{\mathrm{jet}}}{\mathrm{d}p_{\mathrm{T,jet}}\mathrm{d}\eta}}, \quad (2)$$

where $\frac{\mathrm{d}^2 N_{\mathrm{AA}}^{\mathrm{jet}}}{\mathrm{d}p_{\mathrm{T,jet}}\mathrm{d}\eta}$ is jet yield in the nucleus+nucleus collision, scaled by the number of analysed events $N_{\mathrm{evt}}^{\mathrm{AA}}$, $\frac{\mathrm{d}^2 N_{pp}^{\mathrm{jet}}}{\mathrm{d}p_{\mathrm{T,jet}}\mathrm{d}\eta}$ is the yield measured in the $p+p$ collisions, scaled by the corresponding events N_{evt}^{pp}. The $p+p$ spectra are scaled by the average number of binary collisions $\langle N_{\mathrm{coll}} \rangle$ calculated from the Glauber model.

Figure 3 presents a comparison of the measured charged-particle jet R_{AA} to various theoretical calculations. The reference distribution is given by the inclusive charged-particle jet spectrum in $p+p$ collisions at $\sqrt{s} = 200$ GeV, as calculated using PYTHIA. The Hybrid [6], LBT [7], and LIDO [8,9] models provide predictions for charged-particle jets, while the SCET [10,11] and NLO pQCD calculations [12] correspond to fully reconstructed jets. Since the $p_{\mathrm{T,jet}}$ dependence of full jet R_{AA} is weak, a comparison between these calculations and the charged-particle jet data remains meaningful. Additionally, the LBT and LIDO models incorporate a cut on the leading constituent in the Au+Au spectrum, consistent with the $p_{\mathrm{T,lead}}^{\mathrm{min}} = 5$ GeV$/c$ requirement applied in the experimental analysis. All theoretical predictions are found to be consistent with the measured inclusive jet R_{AA} within uncertainties in the unbiased kinematic region. The most significant differences among models appear for $R = 0.4$, indicating that ongoing measurements of inclusive jet R_{AA} may have the potential to distinguish between these theoretical approaches.

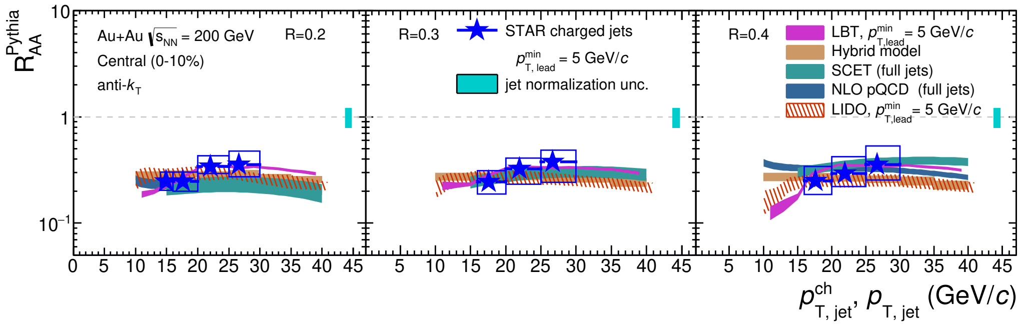

Figure 3. Comparison of R_{AA} (stars) measured in the Au+Au collisions at $\sqrt{s_{\mathrm{NN}}} = 200$ GeV to the theoretical calculations. The Hybrid [6], LBT [7], and LIDO [8,9] calculations correspond to charged-particle jets, while SCET [10,11] and the NLO [12] calculations refer to fully reconstructed jets. Taken from Ref. [5].

3.2. Semi-inclusive Recoil Jet Yield Modification

A powerful tool to investigate the properties of the QGP is the study of jets recoiling from high transverse energy (E_{T}) direct photons (γ_{dir}) [13]. Since γ_{dir} photons do not undergo strong interactions with the medium, they provide a clean probe of jet quenching effects. Furthermore, comparing measurements of γ_{dir}+jet and π^0+jet events can offer insights into the color factor and path-length dependence of energy loss mechanisms [14]. The study of recoil jet distributions for different jet cone radii also serves as a sensitive probe of in-medium jet broadening.

In this section, an analysis of fully-corrected, semi-inclusive distributions of charged-particle jets recoiling from high-E_T γ_{dir} and π^0 triggers in central Au+Au collisions at $\sqrt{s_{NN}} = 200$ GeV is reported. The dataset was collected during the 2014 RHIC run, utilizing a trigger condition that required an energy deposition greater than 5.6 GeV in a single tower of the STAR Barrel Electromagnetic Calorimeter (BEMC).

A variable similar to the nuclear modification factor is defined for the semi-inclusive collisions. This variable I_{AA} is defined as

$$I_{AA} = \frac{Y^{A+A}\left(p_{T,jet}^{ch}, R\right)}{Y^{p+p}\left(p_{T,jet}^{ch}, R\right)}, \tag{3}$$

and compares trigger-normalized jet yields in recoil acceptance for nucleus + nucleus collisions $Y^{A+A}\left(p_{T,jet}^{ch}, R\right)$ and $p + p$ collisions $Y^{p+p}\left(p_{T,jet}^{ch}, R\right)$.

Figure 4 presents the I_{AA} observable, defined as the ratio of the recoil jet yield distributions in central Au+Au collisions to those of $p + p$ collisions, for a common trigger selection and jet resolution parameter R, shown for the highest measured E_T^{trig} bin for each trigger type. A significant suppression of recoil jet yields is observed in central Au+Au collisions for $R = 0.2$, while the suppression is noticeably reduced for $R = 0.5$. The suppression ($I_{AA} < 1$) results from a combination of the spectrum shape effects [15] and population-averaged parton energy loss. The reduced suppression for larger R suggests that a greater fraction of the jet's initial energy is recovered within a cone of radius 0.5 compared to 0.2, providing insight into the angular scale of energy redistribution due to jet quenching.

I_{AA} is consistent within uncertainties for recoil jets triggered by both direct photons (γ_{dir}) and π^0 mesons within the same E_T^{trig} bin, despite the steeper spectrum associated with π^0 triggers. This observation indicates a larger average medium-induced energy loss for recoil jets associated with π^0 triggers, offering new constraints on the flavor and path-length dependence of jet quenching mechanisms [15].

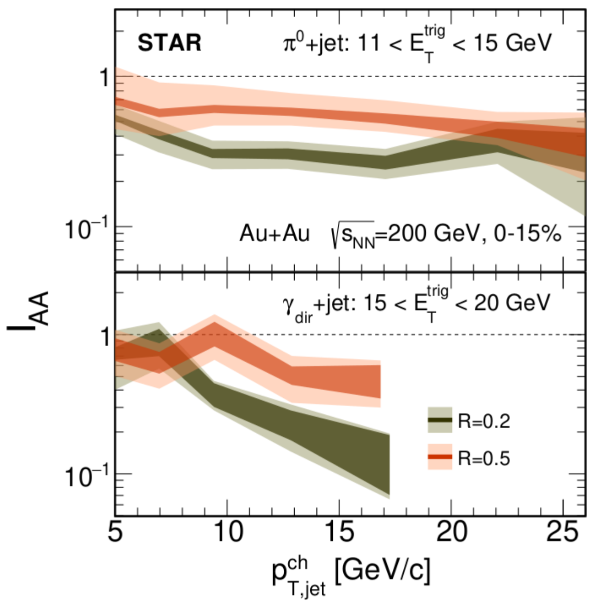

Figure 4. The I_{AA} of semi-inclusive recoil jet distributions in central Au+Au collisions at $\sqrt{s_{NN}} = 200$ GeV shown for both γ_{dir} and π^0 triggers, with $R = 0.2$ and $R = 0.5$. The uncertainty bands reflect the correlated uncertainties in both the numerator and denominator. The dark bands indicate statistical uncertainties, while the light bands represent systematic uncertainties.

3.3. Semi-inclusive Yield Modification in p+Au Collisions

In contrast to Au+Au collisions, where event activity (EA) or centrality is typically classified based on charged particle multiplicity at midrapidity [16], defining a centrality proxy in small systems like $p+$Au is more challenging due to significant contributions from hard scatterings, which introduce autocorrelations between jet production and the EA measurement. To mitigate this, a large separation in pseudorapidity between the EA measurement and midrapidity jets is required.

In this analysis, STAR utilizes the Beam-Beam Counters located in the Au-going direction, covering $\eta_{\mathrm{BBC}} \in [-5, -3.4]$, to quantify EA based on the sum of ADC signals from scintillating tiles. This method provides a wide rapidity gap relative to jets measured at $|\eta| \leq 0.6$, effectively reducing autocorrelation effects. The EA distribution measured by the BBC is used to classify events into low- and high-EA categories, defined respectively as the lowest and highest 30% of the minimum bias EA distribution. Despite detector signal saturation effects, correlations between EA measured by the BBC and midrapidity charged particle density confirm the suitability of this method as a centrality proxy in $p+$Au collisions.

Figure 5 presents the first fully-corrected semi-inclusive jet spectra in small system collisions at RHIC. The jet spectra per trigger are shown for both trigger-side and recoil-side jets, with an azimuthal selection of $\Delta\phi < \pi/3$ around the trigger direction or opposite to it for recoil jets. A clear suppression of both trigger- and recoil-side jet yields is observed in high-EA events compared to low-EA events. Notably, the suppression is comparable for both sides, which differs from typical jet quenching signatures in large systems, where recoil-side jets are more strongly suppressed. This suggests that the observed suppression in small systems may arise from correlations between event activity and the underlying hard scattering scale, rather than genuine in-medium energy-loss effects.

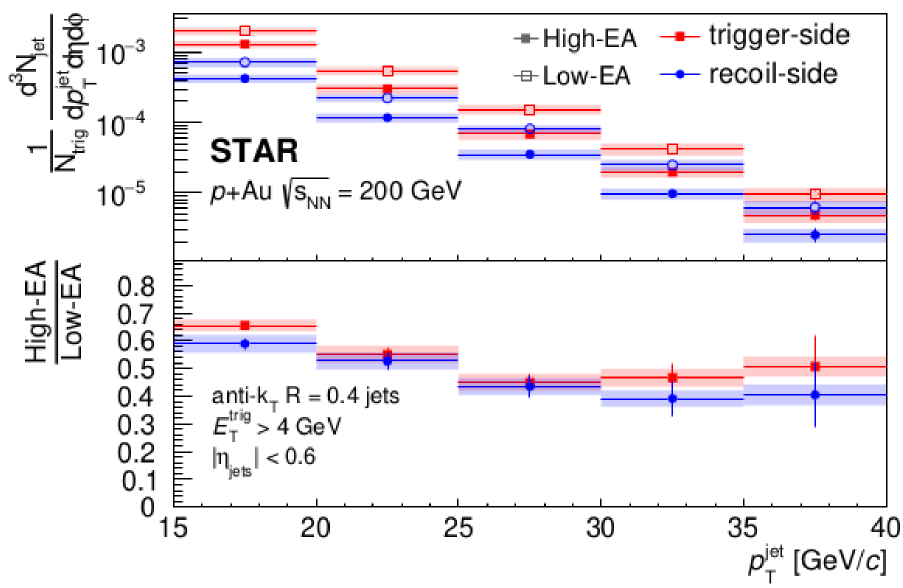

Figure 5. Jet spectra per trigger for the trigger-side ($|\phi_{\mathrm{jet}} - \phi_{\mathrm{trig}}| < \pi/3$) and recoil-side ($|\phi_{\mathrm{jet}} - \phi_{\mathrm{trig}}| > 2\pi/3$) jets are shown in the top panel. Jets are reconstructed with $R = 0.4$, and the offline trigger requirement is $E_{\mathrm{T}}^{\mathrm{trig}} > 4$ GeV. Spectra are presented for both high-EA and low-EA event classes. The bottom panel shows the ratio of semi-inclusive jet spectra in high-EA to low-EA events. Statistical uncertainties are represented by the error bars, while systematic uncertainties are indicated by the shaded boxes. Taken from [17].

4. Conclusions

Jets serve as an essential probe for studying in-medium energy loss in nucleus-nucleus collisions. The STAR experiment observes a significant suppression of jet yields in Au + Au collisions, consistent with strong interactions of jets with the quark-gluon plasma. In contrast, no significant suppression is observed in p + Au collisions. Future measurements based on new datasets with larger statistics will provide improved precision, extended kinematic reach, and enhanced capabilities for full jet reconstruction.

Acknowledgments: The work has been supported by the Czech Science Foundation grant 23-07499S

References

1. Tannenbaum, M. J. (2019). Latest Results from RHIC Progress on Determining $\hat{q}L$ in RHI Collisions Using Di-Hadron Correlations. *Universe*, *5*(6). https://doi.org/10.3390/universe5060140
2. ALICE Collaboration (2014). Measurement of charged jet suppression in Pb-Pb collisions at $\sqrt{s_{\rm NN}}$ = 2.76 TeV. *Journal of High Energy Physics*, *2014*(3). https://doi.org/10.1007/JHEP03(2014)013
3. STAR Collaboration (2003). Transverse-Momentum and Collision-Energy Dependence of High-$p_{\rm T}$ Hadron Suppression in Au+Au Collisions at Ultrarelativistic Energies. *Physical Review Letters*, *91*(17). https://doi.org/10.1103/PhysRevLett.91.172302
4. ATLAS Collaboration (2015). Measurement of charged-particle spectra in Pb-Pb collisions at $\sqrt{s_{\rm NN}}$ = 2.76 TeV with the ATLAS detector at the LHC. *Journal of High Energy Physics*, *2015*(9). https://doi.org/10.1007/JHEP09(2015)050
5. STAR Collaboration (2020). Measurement of inclusive charged-particle jet production in Au+Au collisions at $\sqrt{s_{\rm NN}}$ = 200 GeV. *Physical Review C*, *102*(5). https://doi.org/10.1103/PhysRevC.102.054913
6. Casalderrey-Solana, J., Hulcher, Z., Milhano, G., Pablos, D., Rajagopal, K. (2019). Simultaneous description of hadron and jet suppression in heavy-ion collisions. *Physical Review C*, *99*(5). https://doi.org/10.1103/PhysRevC.99.051901
7. He, Y., Cao, S., Chen, W., Luo, T., Pang, L. -G., Wang, X. -N. (2019). Interplaying mechanisms behind single inclusive jet suppression in heavy-ion collisions. *Physical Review C*, *99*(5). https://doi.org/10.1103/PhysRevC.99.054911
8. He, Y., Luo, T., Wang, X. -N., Zhu, Y. (2015). Linear Boltzmann transport for jet propagation in the quark-gluon plasma: Elastic processes and medium recoil. *Physical Review C*, *91*(5). https://doi.org/10.1103/PhysRevC.91.054908
9. Ke, W., Xu, Y., Bass, S. A. (2019). Modified Boltzmann approach for modeling the splitting vertices induced by the hot QCD medium in the deep Landau-Pomeranchuk-Migdal region. *Physical Review C*, *100*(6). https://doi.org/10.1103/PhysRevC.100.064911
10. Chien, Y. -T., Emerman, A., Kang, Z. -B., Ovanesyan, G., Vitev, I. (2016). Jet quenching from QCD evolution. *Physical Review D*, *93*(7). https://doi.org/10.1103/PhysRevD.93.074030
11. Chien, Y. -T., Vitev, I. (2016). Towards the understanding of jet shapes and cross sections in heavy ion collisions using soft-collinear effective theory. *Journal of High Energy Physics*, *2016*(5). https://doi.org/10.1007/JHEP05(2016)023
12. Vitev, I., Zhang, B. -W. (2010). Jet Tomography of High-Energy Nucleus-Nucleus Collisions at Next-to-Leading Order. *Physical Review Letters*, *104*(13). https://doi.org/10.1103/PhysRevLett.104.132001
13. Wang, X. -N., Huang, Z., Sarcevic, I. (1996). Jet Quenching in the Direction Opposite to a Tagged Photon in High-Energy Heavy-Ion Collisions. *Physical Review Letters*, *77*(2), 231-234. https://doi.org/10.1103/PhysRevLett.77.231
14. STAR Collaboration (2016). Jet-like correlations with direct-photon and neutral-pion triggers at $\sqrt{s_{\rm NN}}$ = 200 GeV. *Physics Letters B*, *760*, 689-696. https://doi.org/10.1016/j.physletb.2016.07.046
15. STAR Collaboration (2023). Semi-inclusive direct photon+jet and π^0+jet correlations measured in $p + p$ and central Au+Au collisions at $\sqrt{s_{\rm NN}}$ = 200 GeV. arXiv:2309.00145 [nucl-ex].
16. Miller, M. L., Reygers, K., Sanders, S. J., Steinberg, P. (2007). Glauber Modeling in High-Energy Nuclear Collisions. *Annual Review of Nuclear and Particle Science*, *57*(1), 205-243. https://doi.org/10.1146/annurev.nucl.57.090506.123020
17. STAR Collaboration (2024). Correlations of event activity with hard and soft processes in p+Au collisions at $\sqrt{s_{\rm NN}}$ = 200 GeV at the RHIC STAR experiment. *Physical Review C*, *110*(4). https://doi.org/10.1103/PhysRevC.110.044908